A Numerical Study on Effects of Land-Surface Heterogeneity from 'Combined Approach' on Atmospheric Process Part II: Coupling-Model Simulations①

Zeng Xinmin (曾新民), Zhao Ming (赵 鸣), Su Bingkai (苏炳凯)

Department of Atmospheric Sciences, Nanjing University, Nanjing 210093

(Received February 1, 1999; revised July 16, 1999)

ABSTRACT

Two land surface schemes, one the standard Biosphere / Atmosphere Transfer Scheme Version le (B0Z) and the other B1Z based on B0Z and heterogeneously-treated by 'combined approach', were coupled to the meso-scale model MM4, respectively. Through the calculations of equations from the companion paper, parameters representing land surface heterogeneity and suitable for the coupling models were found out. Three cases were simulated for heavy rainfalls during 36 hours, and the sensitivity of short-term weather modeling to the land surface heterogeneity was tested. Through the analysis of the simulations of the three heavy rainfalls, it was demonstrated that B1Z, compared with B0Z, could more realistically reflect the features of the land surface heterogeneity, therefore could more realistically reproduce the circulation and precipitation amount in the heavy rainfall processes of the three cases. This shows that even short-term weather is sensitive to the land surface heterogeneity, which is more obvious with time passing, and whose influence is more pronounced in the lower layer and gradually extends to the middle and upper layer.

Through the analysis of these simulations with B1Z, it is suggested that the bulk effect of smaller-scale fluxes (i.e., the momentum, water vapor and sensible heat fluxes) near the significantly-heterogeneous land surface is to change the larger-scale (i.e., meso-scale) circulation, and then to influence the development of the low-level jets and precipitation. And also, the complexity of the land-atmosphere interaction was shown in these simulations.

Key words: Combined approach, Land surface heterogeneity, Coupling model, Numerical experiment

1. Introduction

In the companion paper (hereafter referred to as Z99), we combined the mosaic approach and the analytical type of statistical—dynamical approach, and proposed a "combined approach", which could represent both interpatch variability and intrapatch variability as well as computationally cost less. After the heterogeneity of the roughness length z_0 (or / and zero plane displacement height d_0) is considered by the combined approach in Biosphere / Atmosphere Transfer Scheme Version 1e (BATS le) (Dickinson et al., 1993), expressions, such as drag coefficient and snow coverage which are affected by z_0, were obtained. We chose a function $y(y = ln[(z_1 - d_0) / z_0]$, where z_1 is the height of the lowest level in the atmospheric model) of the roughness length z_0 as the probability density function (PDF) (linear and symmetric as Giorgi, 1997a, 1997b) independent variable, and carried out sensitivity experiments against different values of the two parameters, width ratio α_n and height ratio γ of PDF. These experiments, which are the basis of this paper, were aimed at relevant characteristic quantities

①This work was supported by the NKBRSF Project G 1999043400 and the CNSF Project 49735180.

instead of the weather processes or climate states. The main objective of the treatment of land surface heterogeneity is to quantitatively and realistically represent the heterogeneity or the pronounced nonlinear interactions among land surface characteristic quantities and between characteristic quantities at the land surface and those near the surface. Nevertheless, it is far from sufficient to actually reflect the interactions only by the use of stand-alone (or off-line) experiments for land surface models, i.e., it is very necessary for a land surface model to be coupled to an atmospheric model (general circulation model, regional climate model, or weather model).

There are a lot of previous studies on the treatment of land surface heterogeneity. Most of these studies apply the mosaic approach to consider interpatch variability (Deardorff, 1978; Avissar and Pielke, 1989; Koster and Suarez, 1992, Dickinson et al., 1993; Seth et al., 1994; Leung and Ghan, 1995; Wei and Fu, 1997); some use the numerical type of statistical—dynamical approach to consider intrapatch variability (Avissar, 1992; Famiglietti and Wood, 1994; Sivapalan and Wood, 1995; Li and Avissar, 1994); only a few employ the analytical type of statistical—dynamical approach to consider intrapatch variability (Moore and Clarke 1981; Entekhabi and Eagleson, 1989; Giorgi, 1997a; Giorgi, 1997b). Because it is hydrologists who firstly introduced the statistical—dynamical approach, whose numerical type is also computationally expensive, very seldom work has been internationally reported concerning the coupling of a land surface model considering intrapatch variability with an atmospheric model up until now. The studies mentioned above with the inclusion of both interpatch variability and intrapatch variability are all limited to stand-alone experiments of the local land surface.

In this paper, we carried out the experiments of the coupling land-atmosphere model, in which the meso-scale model MM4 developed by Pennsylvania State University and National Center for Atmospheric Research (US) was adopted as the atmospheric component. The data used here are the observed ones from the meteorological stations in the Meiyu season of the summer 1991. For each simulation, the simulating time was less than 36 hours so as to investigate the effects on the short-term weather process due to the land surface heterogeneity represented as Z99. There have been some studies (Anthes, 1984; Beljaars et al., 1996; Wu and Raman, 1997) which have demonstrated the effects of land surface processes on the meso-scale circulation or convective precipitation, while in this paper the effects of land surface heterogeneity are stressed. For saving space here only the roughness-length heterogeneity is studied, while the simulated results of the heterogeneity of stomatal resistance, temperature and moisture will be given in a future paper.

2. Design of experiments

2.1 *Design of the model mesh*

The simulated domain center is located at 35.20°N, 117.00°E, the horizontal grid resolution is 60 km × 60 km, the number of the horizontal grid points is 41 × 40; the domain covers the region of 24.7—45.7°N and 100.88— 133.12°E; in the vertical direction 11 integral levels which are not uniform are set: $\sigma = 0.0, 0.15, 0.30, 0.45, 0.60, 0.75, 0.85, 0.93, 0.97, 0.99, 1.00$; 10 half levels, at which the calculated variables apart from the vertical velocity are output, are located among 11 integral levels.

2.2 *Option of the model physics*

In order to investigate the effects on the short-term weather process due to the land surface heterogeneity represented by the combined approach, for each simulation of a specific period (i.e., from 0000UTC June 12 to 0000TUC June 13 in 1991), two models, the standard version of BATS1e (B0Z) and B1Z which is based on B0Z and treated as Z99, are used. In addition, uniform options of the model physics are adopted so as to make comparisons among the experiments:

(1) Planetary boundary-layer scheme: high-resolution boundary-layer model of Holtslag (Holtslag et al., 1990; Holtslag et al., 1993).

(2) Lateral boundary scheme: time-dependent, exponentially nudging boundary scheme.

(3) Cumulus parameterization scheme: modified Kuo-type scheme (Anthes et al., 1987).

(4) Scheme for water vapor calculation: implicit vapor scheme.

(5) Scheme for radiation transfer: the scheme as CCM2 (Briegleb, 1992).

2.3. *Selection of PDF (probability density function) parameters*

As stated in Z99, the chosen PDF parameters should be relatively consistent with the used model and the properties of the simulated domain, and when testing against PDF parameters, width ratio α_n and height ratio γ, α_n has an upper limit which is generally smaller than about 0.6. Because the value of the chosen γ does not lead to physical mistakes (e.g., the value of the heterogeneous characteristic exceeds the reasonable range), here we only discuss the choosings of width ratios corresponding to y, the single valued function of the roughness length z_0, and corresponding to the stomatal resistance r_s, when performing simulations of the coupling model.

Table 1. Experiments of PDF parameter-choosing in the coupling model. PDF here directly corresponds to y which is a single valued function of z_0), where $z_1 = 38.4$ m, $d_{00} = 9$

No.	α_n	γ	C_{DN0}	z_{00} (m)	z_{0min} (m)	z_{0max} (m)	C_{DN1}	z_{01} (m)	r_{cdn}	r_{z0}
1	0.2	0.001	1.251×10^{-2}	1.00	5.75×10^{-1}	1.60	1.28×10^{-2}	1.34	1.02	1.34
2	0.4	0.001	1.251×10^{-2}	1.00	3.13×10^{-1}	2.31	1.36×10^{-2}	1.47	1.09	1.47
3	0.6	0.001	1.251×10^{-2}	1.00	1.65×10^{-1}	2.98	1.55×10^{-2}	1.63	1.24	1.63
4	0.2	0.9	1.251×10^{-2}	1.00	5.75×10^{-1}	1.60	1.30×10^{-2}	1.05	1.04	1.05
5	0.4	0.9	1.251×10^{-2}	1.00	3.13×10^{-1}	2.31	1.48×10^{-2}	1.13	1.18	1.13
6	0.6	0.9	1.251×10^{-2}	1.00	1.65×10^{-1}	2.98	1.93×10^{-2}	1.25	1.54	1.25
7	0.2	0.001	1.065×10^{-2}	0.80	4.26×10^{-1}	1.38	1.09×10^{-2}	0.98	1.02	1.23
8	0.4	0.001	9.865×10^{-3}	0.71	1.79×10^{-1}	2.04	1.08×10^{-2}	0.98	1.09	1.38
9	0.6	0.001	8.765×10^{-3}	0.58	5.92×10^{-2}	2.74	1.09×10^{-2}	0.99	1.24	1.71
10	0.2	0.9	1.205×10^{-2}	0.95	5.38×10^{-1}	1.55	1.25×10^{-2}	1.00	1.04	1.05
11	0.4	0.9	1.103×10^{-2}	0.84	2.34×10^{-1}	2.17	1.31×10^{-2}	0.98	1.19	1.17
12	0.6	0.9	1.025×10^{-2}	0.76	9.55×10^{-2}	2.85	1.58×10^{-2}	1.04	1.55	1.37

Table 1 shows the experimental results of PDF parameter choosing in the coupling model, where α_n, γ, z_{00}, z_1 and d_{00} are the inputs, the others are output results; d_{00} is the ratio of zero plane displacement to z_0; C_{DN0} and z_{00} are the drag coefficient and the roughness length without the heterogeneity treatment; C_{DN1} and z_{01} which are appended with subscript "1" denote the drag coefficient and the roughness length with the heterogeneity treatment,

respectively; r_{cd0} and r_{z0} are the ratios of the drag coefficient and the roughness length with heterogeneity treatment to their corresponding values; z_{0min} and z_{0max} are the lower and upper limits of z_0 after the heterogeneity treatment, respectively.

From Table 1, some conclusions analogous to Z99 can be drawn, say, the average of the roughness length will increase after the heterogeneity treatment (i.e., $r_{z0} > 1$). Since values of z_{00}, z_1 and d_{00} are close to those inputs in standard BATS1e (B0Z) in the case of vegetations, under the condition assuming roughness length z_0, which was classified by Olson et al. (1983) with respect to vegetations, to be a specific average (even though it is very approximate), in order to make z_{01} (a value for z_0 after heterogeneity treatment) approximate to z_0 given by classification, the ratio c_{00} of the input z_{00} to z_0 must be within the range from 0.6 to 0.95. Based on all these, the heterogeneity is considered. For example, in the 9th row of Table 1, $z_{01} = 0.99$ m, which is close to the classification $z_0 = 1$ m, when $z_{00} = 0.58$ m. So for the original classification $z_0 = 1$ m, we input $z_{00} = 0.58$ m. On the basis of this we change z_0 in B0Z into other value in B1Z, and then use the changed value to calculate the heterogeneously-treated values of the expressions of relevant characteristic quantities such as the drag coefficient, snow coverage, etc.

The heterogeneity of stomatal resistance r_s is also considered in simulations with the coupling model. Since there are many factors which are very complicated and affect r_s, the spatial distribution of r_s is highly heterogeneous, there are a lot of controversies about r_s treatments in the land surface models (Carlson, 1991), most of the r_s equations are given empirically (Avissar,1993), and the minimum r_s in B0Z produced too low evaporation and too high sensible heat flux compared to observations (Giorgi, 1997b). In this paper, the output value of the B0Z algorithm is used as the average in the distribution, with the r_s PDF similar to y, and its width ratio $\alpha_n \leqslant 0.30$.

3. Simulations and analysis

Heavy rainfalls (daily precipitation amount $\geqslant$ 100 mm) in the Meiyu season are the main disastrous weathers in China and the subtropical region in Japan. This kind of weather is often associated with a Meiyu front, which is quasi-stationary and separates two intensive air masses, in which one is very warm and humid and comes from the tropical Pacific Ocean in the south, and the other is relatively cold and comes from the north, therefore the precipitation is concentrated in a relatively narrow and limited latitude belt and turns out to be very strong.

Great losses in economy were caused by the long-time rainfall in East China in the summer of 1991, when the onset time of the Meiyu season was early at the end of May, and when the Meiyu season lasted for a very long period with its ending in the early July. Here three cases are chosen in the year: the first (hereafter referred to as case 1) from 0000UTC June 12 to 0000UTC June 13, the second (case 2) from 1200UTC July 4 to 1200UTC July 5, and the third (case 3) from 0000UTC May 24 to 1200UTC July 25. All of the observations for the three cases are utilized for modeling and analysis so as to test the sensitivity of the short-term weather to the land process model B1Z.

We select several sets of parameters listed in Table 2 for the tests, and the following is the analysis.

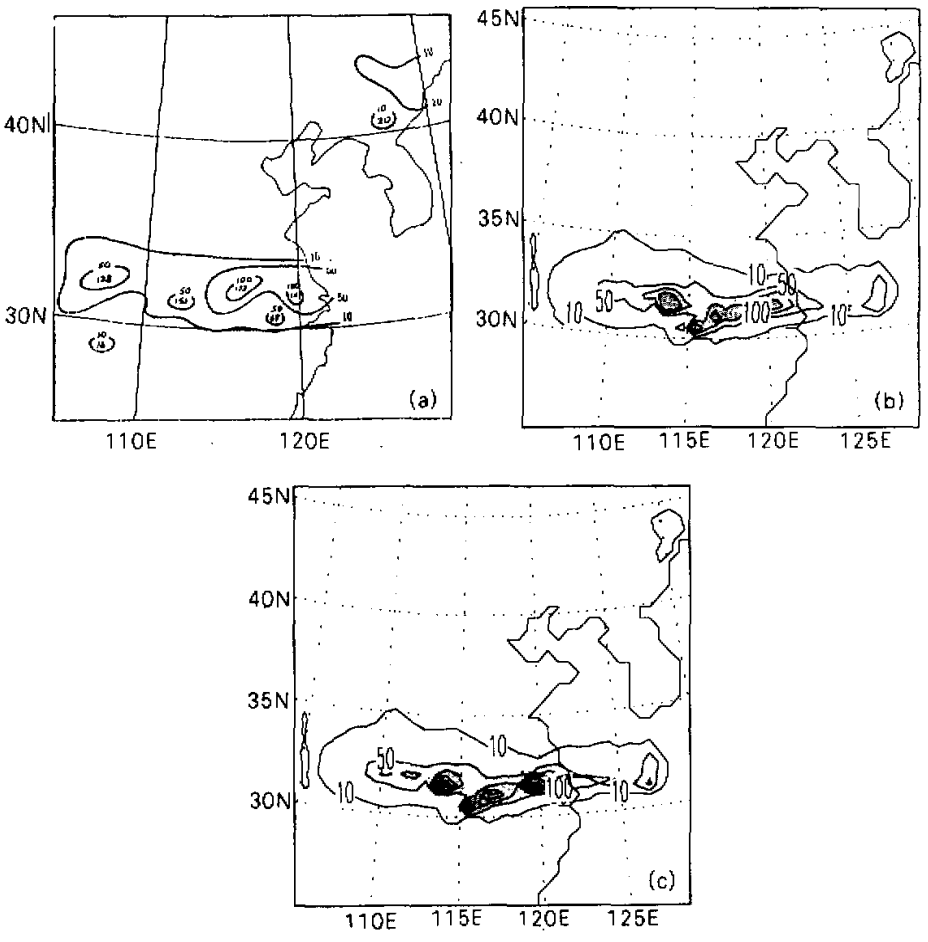

Fig. 1. Observed (a) and simulated in Exp.1 (b) and Exp.2 (c) daily precipitation amounts (in mm) from 0000UTC on June 12 to 0000UTC on June 13, 1991.

3.1 *Analysis of Exp.1 and Exp.2*

Around June 12 was the active season of the Meiyu front, when the real weather situations were as follows: There existed a quasi-longitudinal Meiyu front in the surface weather map in 33–35°N at 0000UTC, June 12, and correspondingly, there was unitarily southwest warm and humid air flow in front of the trough (or to the south of the shear line) in the lower layer; up to 1200UTC, the Meiyu front moved for about 5° latitude in the SSE direction, in this period little troughs rapidly moved eastward at 500 hPa, and intensified the anti-cyclone circulation in the north of the frontal zone; later Meiyu front was quasi-stationary (not shown). At that time a great disaster was caused by the heavy rainfall in the Yangtze River–Huaihe River Valley, where the maximum precipitation from 0000UTC June 12 to 0000UTC June 13 reached 172 mm (see Fig. 1a). Exp.1 and Exp.2 simulate the case (case 1),

in which Exp.1 uses the coupling model with B1Z included and with its parameters selected as Table 2, while Exp.2 employs B0Z. The same boundary condition is chosen for the two experiments, whose difference only exists in whether the heterogeneity treatment by the combined approach is considered or not.

It is well known that the influence of initial conditions is greater than that of boundary conditions for short-term weather processes. The influence of boundary conditions may be obvious only a long time later. Hence, there is little difference between the characteristic quantities of the two experiments in a short period of integration.

Table 2. Selection of the parameters and results of simulation. (Parameters in the functional form of the heterogeneous independent variable correspond to r_s and y; n_{10}, n_{100}, n_{230} are the numbers of the grid cells in which precipitation amount is greater than 10, 100, 230 mm, respectively; P_s and P_o are the maximum daily precipitation amounts simulated and observed in the Yangtze River-Huaihe River Valley, respectively, both in mm)

	input parameter						simulated value				observed value
Exp.(model)	$\alpha_n(y)$	$\gamma(y)$	$\alpha_n(r_s)$	$\gamma(r_s)$	d_{00}	c_{00}	n_{10}	n_{100}	n_{230}	P_s	P_o
Exp.1 (B1Z)	0.5	0.9	0.3	0.001	9	0.6	211	22	0	229	172
Exp.2 (B0Z)	–	–	–	–	–	–	216	23	5	288	172
Exp.3 (B1Z)	0.01	0.001	0.01	0.001	9	1	216	21	5	284	172
Exp.4 (B1Z)	0.5	0.9	0.3	0.01	9	1	208	21	4	257	172
Exp.5 (B1Z)	0.25	0.9	0.3	0.006	9	0.6	188	18	0	164	157
Exp.6 (B0Z)	–	–	–	–	–	–	190	19	0	175	157
Exp.7 (B1Z)	0.15	0.9	0.3	0.006	9	0.9	460	2	0	142	173
Exp.8 (B0Z)	–	–	–	–	–	–	458	5	0	119	173

After 0900UTC, the difference between the two experiments becomes apparent gradually. At 0900UTC, the sensible heat flux in Exp.1 is greater than that in Exp.2 over almost the whole region, the corresponding 3-hour (0600-0900UTC) accumulated sensible heat flux is also greater than that in Exp.2, while the difference between the latent heat fluxes in the two experiments is not so apparent (not shown). All these show that much heat is transported from the surface to the atmosphere in Exp.1, which may lead the temperature in the lower layer to be higher than that in Exp.2, therefore it is favorable for the lower layer to be more unstable and intensifies the convective development.

Now compare the observed and simulated temperatures at 1200UTC (not shown). Because of the biases of MM4 (Here we regard the relatively great difference between the results of the observations and simulations in the atmosphere as the "MM4 biases", while take the difference between the two coupling models which employ B1Z and B0Z respectively as the difference affected by the two land surface models. In the analysis of the simulations, we must try our best to distinguish the respective effects of MM4 and the land surface models), the basic characteristics of temperatures simulated by the two experiments are quite consistent with observations, but the results in Exp.1 are closer to those in Exp.2. Over the entire simulated domain, the temperature in Exp.1 is a bit higher than that in Exp.2, which agrees with the above-mentioned transportation of sensible heat. From the viewpoint of time, the lower atmosphere is firstly influenced by the land processes, and later the upper atmosphere is affected by the lower layer one via various dynamical and thermodynamic processes. So, it can be concluded that the lower layer in Exp.1 is more unstable than that in Exp.2. Seen from the

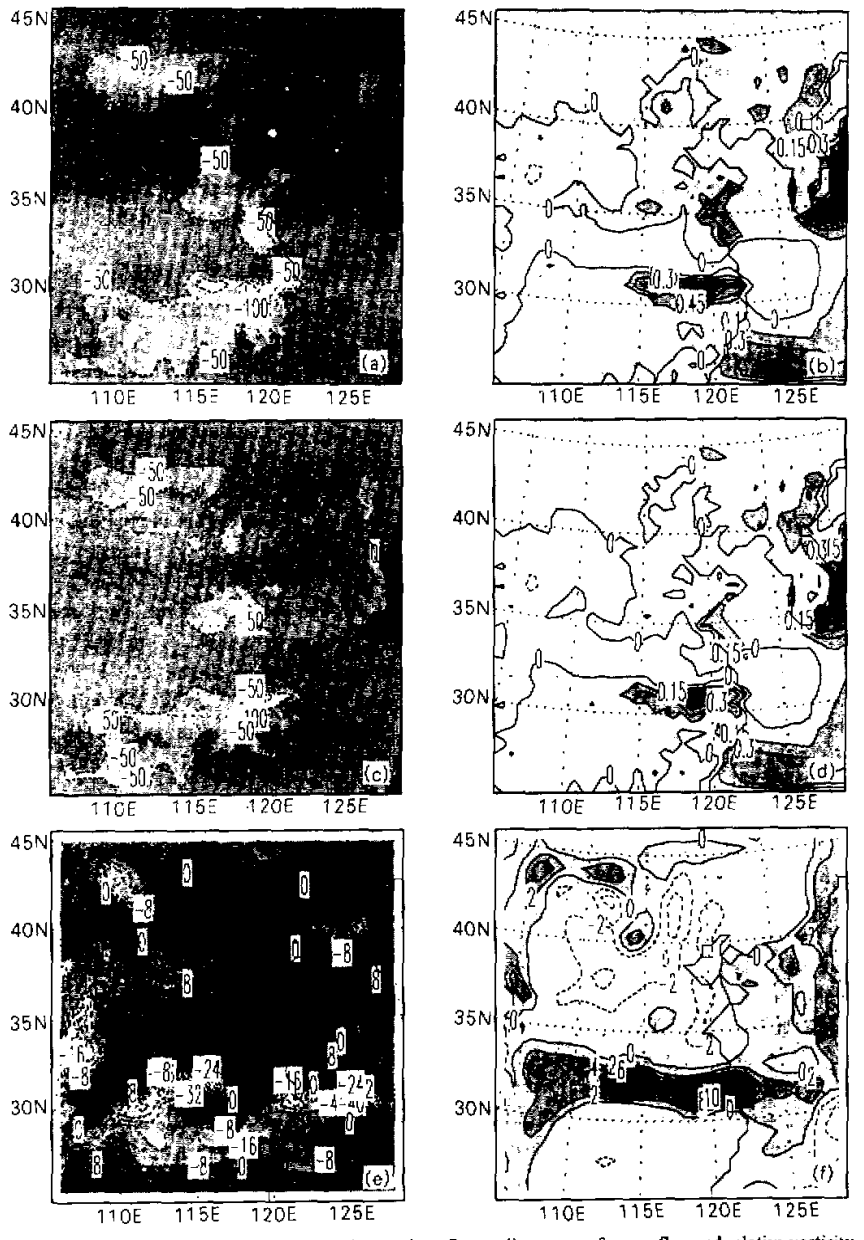

Fig. 2. Simulated land surface sensible heat and latent heat fluxes, divergence of vapor flux and relative vorticity. (a) and (c) are for the land surface sensible heat fluxes (in W/m^2) at 2100UTC June 12 in Exp.1 and in Exp.2 respectively; while (b) and (d) for the surface vapor fluxes (in 10^{-4} m / s) at 2100UTC June 12 in Exp.1 and Exp.2, respectively; (e) for the 850 hPa divergence of vapor flux $\nabla \cdot (q\vec{v})$ (in 10^{-8} / s) at 0000UTC June 13 in Exp.1; (f) for the 850 hPa relative vorticty (in 10^{-5} / s) at 0000UTC June 13 in Exp.2.

observational weather map (not shown), there is a large horizontal gradient of the horizontal wind speeds at point *M* (around 31°N, 118°E), which corresponds to the frontal zone in the lower layer. Besides, there is an SW low level jet (LLJ) whose maximum speed is greater than 14 m/s below 700 hPa in the south of the frontal zone. Both Exp.1 and Exp.2 quite successfully simulated the LLJ location, from which the MM4 bias in modeling the windspeed is shown: the simulated wind speed is greater than the observation. In the space northward from point *M* and below 600 hPa, there is a difference in the wind speed to some extent between the two experiments, which is affected by the land surface models. That is to say, the difference of the circulations between the two experiments becomes more apparent gradually (not shown).

The surface run-off simulated for 2100UTC by different land surface models exhibits quite a difference (not shown). From the two-by-two comparisons of Fig. 2a and Fig. 2c as well as Fig. 2b and Fig. 2d, we can see that, contrary to that at 0900UTC, more sensible heat taken at the ground is simulated in Exp.1, while the evaporation flux is also greater than the corresponding result in Exp.2. All these are consistent with the accumulated sensible heat flux and accumulated latent heat flux for 1800–2100UTC (not shown). The transfer of sensible heat flux makes the temperature in the lower layer decrease in Exp.1, and also decreases the inner energy in the lower layer; while the relatively large evaporation flux means the increase of humid hydrostatic energy in the lower layer. The contributions of the two kinds of fluxes to the atmospheric stability at 2100UTC are opposite, hence it is very difficult to draw a conclusion for the bulk effect on the atmosphere; and when we turn to the presentation of relatively intense sensible heat (while its evaporation is not so obvious) at 0900UTC in Exp.1 and the results that the lower layer temperature makes the lower layer more unstable at 1200UTC in Exp.1; and that the bulk effect of flux transfer at 2100UTC is uncertain while the daily precipitation in Exp.1 is less than that in Exp.2, we can see that the land–atmosphere interaction described by the models is very complex, in which different dynamical and thermodynamic factors may behave in different ways for different periods.

Figs. 3a, 3c and 3e depict the wind fields observed at 0000UTC June 13 and its corresponding simulations in Exp.1 and Exp.2, respectively, and Figs. 3b, 3d and 3f are the corresponding vertical cross-sections of the horizontal wind speeds through point *M*. The coupling models reproduce some basic characteristics of the wind fields, e.g., the LLJ which is over and in the south of the rain-band, the LLJ intensity which is weaker than that at 1200UTC, the anti-cyclone in the north and over the rain-band, as well as the MM4 bias in modeling the wind speed which is greater than the observation in this case. From the further comparison, we can find that Exp.1 simulates better than Exp.2 for the location of the center of the anti-cyclone which is actually around 115°E, 39°N at 850 hPa; the LLJ in Exp.1 is weaker than that in Exp.2. After all, the results simulated in Exp.1 are closer to the observations than those in Exp.2. It is very interesting that the smallwind speed region extending from the lower layer to about 300 hPa presents a relatively strong center in Exp.2 from vertical cross-section, which is far from the observation of circulation, while this phenomenon does not appear in Exp.1. When we review the vertical cross-section of the wind fields simulated for 0000UTC June 12, we can see that the difference between the results simulated by the different models becomes larger and larger with time.

Because of the difference of drag coefficients in B1Z and B0Z, the differences of circulations and temperatures in the lower layer in the two experiments become larger, it results in the significant differences of the convergence fields of water vapor fluxes at 850 hPa for 0000UTC June 13 in the two experiments, and the convergence fields present pronounced heterogeneity in a relatively small scale with respect to the LLJ one (e.g., for Exp.1, see Fig. 2e). Akiyama (1989) utilized GMS infrared digital data to analyze the characteristics of various scales of the Meiyu fronts in July, 1982, and pointed out that the cloud field at 850 hPa was within the range where the macro-scale fields of water vapor fluxes converge ($\nabla \cdot (q\bar{v}) < 0$). In contrast with our experiments (the following two cases are also included), although the convergence of vapor fluxes in the lower layer is the precondition of forming the clouds and triggering the rainfalls, at 850 hPa only the zone of intensive vapor flux convergence (e.g., $|\nabla \cdot (q\bar{v})| > 24 \times 10^{-8}\ s^{-1}$) is located within the rain-band, and only the zone where the simultaneous relative vorticities are greater than $2 \times 10^{-5}\ s^{-1}$ in the field of the relative vorticity (see Fig. 2f) can better correspond to the short-term rain-band.

The observed and simulated daily precipitations are given in Figs. 1a, 1b, 1c, where the rain-band simulated in Exp.1 is better, e.g., its SW corner extending farther away, the locations of several simulated centers of the heavy rainfall as well as their maximum values are closer to observations (i.e., compared with the maximum daily precipitation 288 mm in Exp.2, the maximum daily precipitation in Exp.1 is 229 mm which is closer to the observed 172 mm). Further analysis of the 6-hour precipitations can reveal the complex details (not shown): the area and the intensities of the third and the fourth 6-hour precipitations in the far west part in Exp.1 are all greater than those in Exp.2; while the third 6-hour precipitation in Exp.2 are greater than that in Exp.1 in a greater area, but the fourth 6-hour precipitation in Exp.2 are less than that in Exp.1 in a greater area. Hence, the details of precipitation in each period are not always consistent with the bulk intensity in the whole 24 hours, which further demonstrates the complexity of the land-atmosphere interaction.

The above analysis shows that compared with Exp.2, Exp.1 has more successfully simulated the heavy rainfall from 0000UTC June 12 to 0000UTC June 13. Apparently it is the transportation of various fluxes from the land surface that mainly determines the differences between the two experiments. Because the transportation of various fluxes from the land surface must act by way of the lower layer on the convective precipitation taking place in the middle or upper layer, the flux transportation from the land surface is not the main mechanism of the heavy rainfall. We suggest that the main mechanism should be the LLJ dynamical effects.

It is a significant feature for an LLJ to exist to the south or the southeast of the 850 / 700 hPa trough (or shear line) (Matsumoto et al., 1971; Tao and Chen, 1987), and a close relationship between extremely heavy rainfall or a mesoscale convective system and an LLJ during the Meiyu season has been found all over East Asia (Matsumoto, 1972; Tao and Chen, 1987; Chen et al., 1988). Furthermore, Akiyama (1989) suggested that the wind of the lower layer in the south of the Meiyu front is the main factor in determining the activity of the Meiyu front. Many meteorologists have studied the physical processes for which the LLJ had resulted in heavy rainfalls, e.g., Matsumoto (1972) drew the conclusion that the upward branch of the secondary circulation associated with the LLJ is responsible for the heavy rainfall. Chen, (1977) suggested that the LLJ is the main mechanism for creating potential instability to the warm side of a Meiyu front and for generating the convective heavy rainfall by

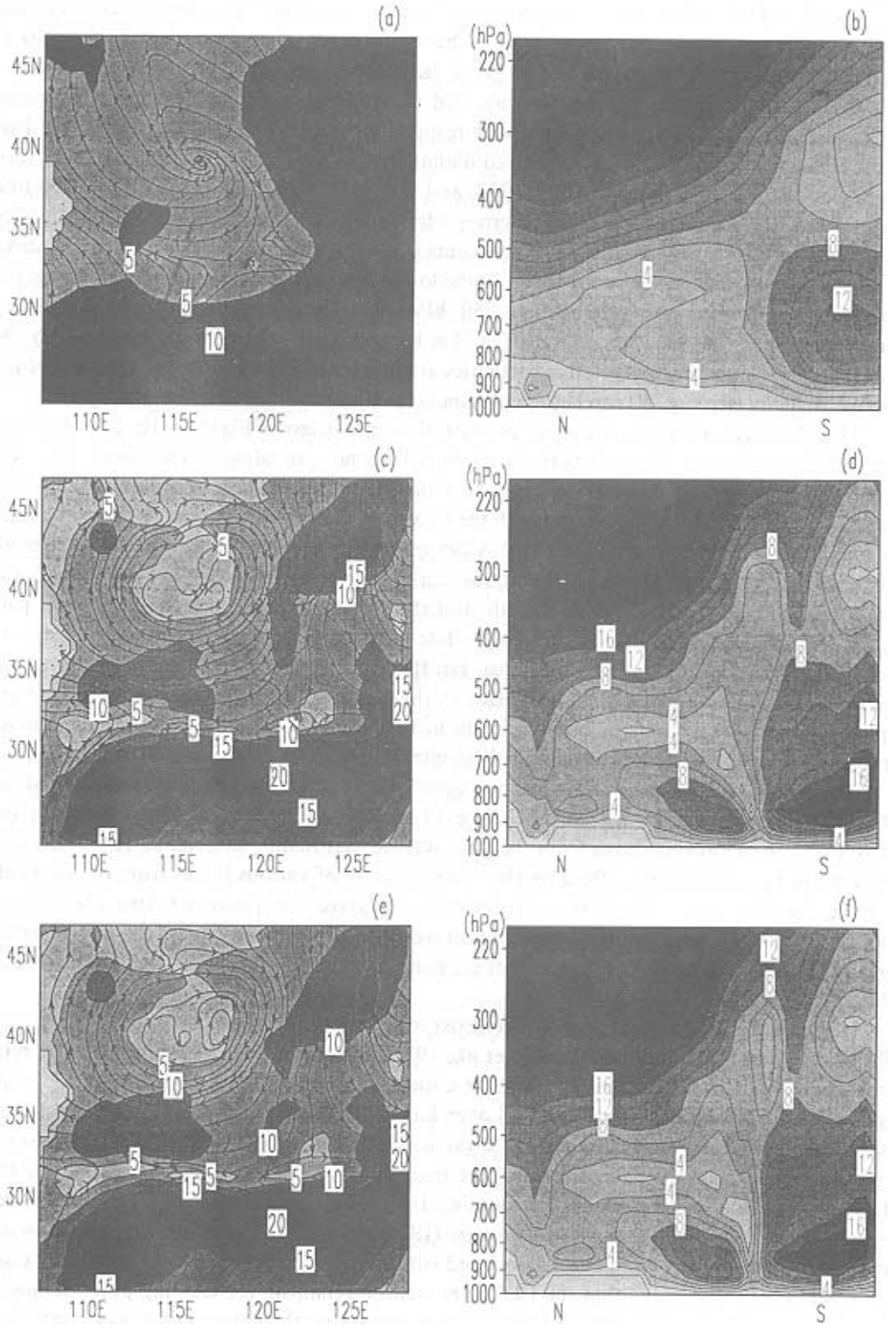

Fig. 3. 850 hPa flow fields, wind fields and vertical cross-sections (NS) through point M (around 118°E, 31°N). (a), (c) and (e) are for the observed, the simulated in Exp.1 and Exp.2 at 0000UTC June 13, respectively; (b), (d) and (f) for the vertical cross-sections corresponding to (a), (c) and (e). All units are in m / s.

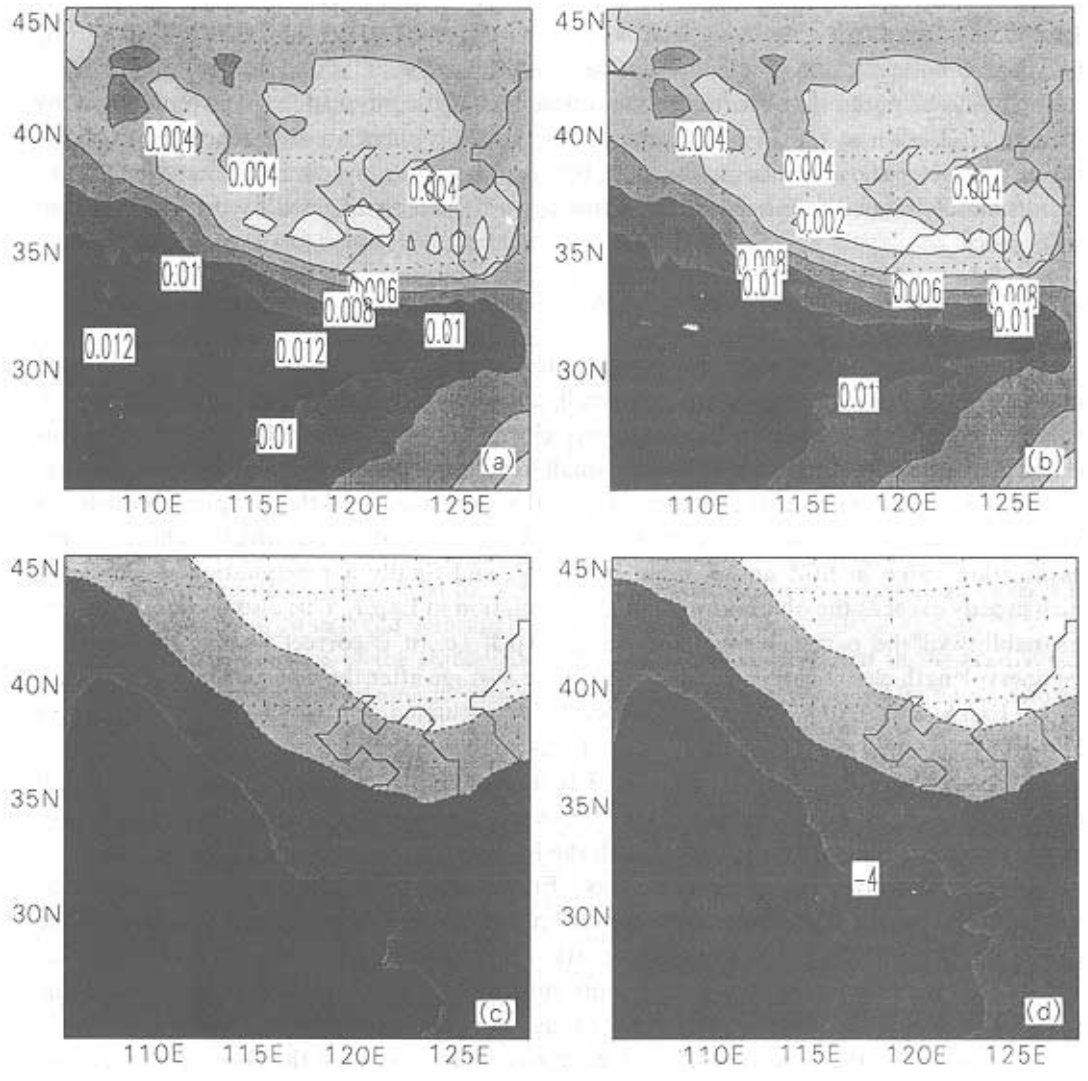

Fig. 4. Simulated specific humidities (interval: 0.002 kg / kg) and temperature (interval: 4°C) at 0000UTC June 13. (a) and (b) are for the 700 hPa specific humidities in Exp.1 and Exp.2, respectively, (c) and (d) for the 500 hPa temperatures corresponding to (a) and (b) respectively.

the associated convergence downstream. Chen (1963) used the thermalwind theory to explain why heavy rainfalls existed in front of the left side of the large-wind center of the LLJ and behind the right side of the upper-level jet.

The observations and simulations for case 1 confirmed the above conclusions of the relationship between LLJs and heavy rainfalls. Analogous to those at 1200UTC June 12, at 0000UTC June 13, the NS vertical cross-sections of the LLJ at a point other than *M* also illustrate that the LLJ simulated in Exp.1 is apparently weaker than that in Exp.2 and closer to the observation (not shown). So we can see the effects of the land surface on the heavy rainfall: the land surface transports upwards the momentum, sensible heat and latent heat, though the influences of these small-scale fluxes in different locations are different in different periods, their bulk effect changes the dynamical and thermodynamic structures (especially

the LLJ) of the relatively-large scale, which further influence the heavy rainfall. In case 1, the LLJ simulated in Exp.1 employing B1Z is closer to the observation than that in Exp.2 using B0Z, therefore the relevant precipitation is better simulated.

It should be noted that because of the differences of the physical features represented by B0Z and B1Z, even in the 24-hour simulations, not only there are differences between the fields of characteristic quantities at 850 hPa, but also the upper layer is influenced (see Fig. 4), which is closely related to intensive convective upward currents affected by the LLJ-induced convergence.

3.2 *Concise analysis of the other experiments*

In order to test the sensitivities of parameters α_n and γ, Exp.3 and Exp.4 are designed (see Table 2). In Exp.3, α_n and γ are very small, d_{00} and c_{00} are chosen as the B0Z input values, and the simulated results in Exp.3 are very close to those in Exp.2. This further confirms the conclusion in Z99 that when α_n is very small, results with the heterogeneity treatment are very close to those without the treatment, via the simulations of the coupling models. In Exp.4, α_n, γ and d_{00} are the same as those in Exp.1, but c_{00} is different which is chosen as the classification value in B0Z and is input into B1Z, and finally a precipitation is simulated which greatly exceeds the observation and the simulation in Exp.1. This also demonstrates the reasonability of the parameter c_{00} selected in Exp.1, i.e., it is correct to take the value of roughness-length classification as the approximate average after the heterogeneity treatment.

In Exp.5 and Exp.6, case 2 is respectively calculated for the heavy rainfall from 1200UTC July 4 to 1200UTC July 5, when it was at the final phase of the Meiyu season for the Valley; while in Exp.7 and Exp.8, case 3 is respectively calculated for the heavy rainfall from 0000UTC May 24 to 1200UTC May 25, when it was at the early phase of the Meiyu season. Similar to that in case 1, there is still the Meiyu front which leads to the weather process of intensive convection in the two cases . From the comparison between the simulated precipitations and the corresponding observation (see Table 2, while figure not shown), the result in Exp.5 by B1Z is closer to the observation than that in Exp.6 by B0Z, except the bias of MM4 that the rain area in the west is quite small. The whole processes in the simulations obtain many results and conclusions similar to case 1, e.g. (not shown), Exp.5 better simulates the LLJ than Exp.6, the difference of the land surface fluxes between the two experiments becomes greater as the time passing, the field of relative vorticity at 850 hPa can well correspond to the short-term rain-band, and so on.

Analogous to above two cases, the simulations of case 3 also exhibit that Exp.7 by B1Z can reproduce results more consistent with the observations than Exp.8 by B0Z (not shown). Table 2 presents some difference of the rain-bands between the two experiments from 0000UTC May 24 to 1200UTC May 25. In case 1, the precipitation simulated in Exp.2 by B0Z is greater than the observation, while the precipitation simulated in Exp.1 by B1Z is less than that in Exp.2; contrary to those in case 1, the precipitation simulated in Exp.8 by B0Z is less than the observation, while the precipitation simulated in Exp.7 by B1Z is greater than that in Exp.8. All these also reveal the effects and the sensitivity of the land surface heterogeneity in the short-term weather processes.

4. Summary and conclusions

In this paper, two land surface schemes, one the standard BATS1e (B0Z) and the other

B1Z based on B0Z and heterogeneously-treated by 'combined approach', were coupled to the mesoscale model MM4, respectively. On the basis of considering the features of the coupling models, we took roughness length z_0 in B0Z which was a classification value as the approximate value after the heterogeneity treatment in B1Z, through the numerical calculations of the formulae in the companion paper (i.e., Z99) to find out suitable heterogeneity-representing parameters α_n and γ, and designed several experiments to compare those without the heterogeneity treatment, so as to test the sensitivity of the short-term weather processes to the land surface heterogeneity.

We have conducted the three-case simulations for heavy rainfalls within 36 hours when it was in the Meiyu season in May, June and July of 1991, and specifically analyzed the simulation of case 1. It was confirmed that B1Z could quite realistically reflect the characteristics of land surface heterogeneity and therefore could more realistically reproduce the circulations and precipitations in the processes of the short-term heavy rainfalls for these three cases, compared with B0Z. This showed that even the 24-hour short-term weather is sensitive to the land surface heterogeneity. The sensitivity became more obvious with time, which was most apparent in the lower layer and whose influences extended to the upper layer gradually. Hence, this provides a way to us for developing and improving the weather-forecasting models, i.e., it should be considered for the numerical weather forecast system to include the land surface model with detailed heterogeneity representation.

Through the analysis of the three-case simulations, we suggest that in the land surface model B1Z, the bulk effect of smaller-scale fluxes (i.e., the momentum, water vapor and sensible heat fluxes) near the significantly heterogeneous land surface is to change the larger-scale, i.e., mesoscale, circulation (e.g., the low-level jets which are closely related to heavy rainfalls), and further influence the development of convection and precipitation. And also, some details in the rainfall processes have been shown, e.g., the intensive convergence of the vapor fluxes in the rain-band; the relative vorticity field at 850 hPa better corresponding to the rain-band; the contributions of the vapor and sensible heat fluxes to the atmospheric stability are different in different periods in the simulations by B1Z, and the difference of the total precipitations simulated by different land surface schemes does not mean the same trend in different periods. All these demonstrate the complexity of land-atmosphere interaction.

In view of the simulations of precipitation amounts, there is quite an improvement after the heterogeneity treatment, but still there are differences between the observations and simulations. This shows that there is a long-term and arduous journey for us to go in developing the numerical models with the inclusion of land surface schemes. These differences come from two aspects in the models. The first is the aspect of atmospheric models. For the short-term weather processes, atmospheric models which describe the laws of the atmospheric motions are more important than land surface schemes. The second is the aspect of land surface schemes. In this aspect, firstly it is very necessary to correctly and quantitatively describe the transfers of fluxes of the momentum, the vapor and the sensible heat at the land surface, secondly it is necessary to realistically represent various heterogeneities. In this paper, we have only considered the roughness-length heterogeneity, while no temperature and moisture heterogeneity is taken into account. In addition, for lack of the data of higher resolutions, only certain values of the parameters α_n and γ are chosen for the sensitivity experiments, while actually the parameters may differ from the grid cells. Because of the length of this paper, the

heterogeneity of stomatal resistance is not further discussed, which will be given in a future paper.

REFERENCES

Akiyama, T., 1989: Large, synoptic and meso scale variations of the Baiu front, during July 1982, Part I: cloud features. *J. Meteor. Soc. Japan*, **67**, 57–81.

Anthes, R. A., 1984: Enhancement of convective precipitation by mesoscale variations in vegetative covering in semiarid regions. *J. Climate. Appl. Meteor.*, **23**, 541–553.

Anthes, R. A., E. Y. Hsie, and Y. H. Kuo, 1987: Description of the Penn State / NCAR Mesoscale Model Version 4(MM4), NCAR Tech. Note, NCAR / TN–283+STR, 66 pp.

Avissar, R., and R. A. Pielke, 1989: A parameterization of heterogeneous land surface for atmospheric numerical models and its impacts on regional meteorology. *Mon. Wea. Rev.*, **117**, 2113–2136.

Avissar, R., 1992: Conceptual aspects of a statistical–dynamical approach to represent landscape sub–grid heterogeneities in atmospheric models. *J. Geophys. Res.*, **97**, 2729–2742.

Avissar, R., 1993: Observations of leaf stomatal conductance at the canopy scale: An atmospheric modeling perspective. *Bound. –Layer Meteor.*, **64**, 127–148.

Beljaars, A. C. M. et al., 1996: The anomalous rainfall over the United States during July 1993: sensitivity to land surface parameterization and soil moisture anomalies. *Mon. Wea. Rev.*, **124**, 362–383.

Briegleb, B. P., 1992: Delta–Eadington approximation for solar radiation in NCAR Community Climate Model. *J. Geophys. Res.*, **97**, 7603–7612.

Carlson, T. N., 1991: Modeling stomatal resistance: an overview of the 1989 workshop of the Pennsylvania State University. *Agric. For. Meteor.*, **54**, 103–107.

Chen Qiushi, 1963: On the formation and the destruction of thermal wind in a simplie baroclinic atmosphere. *Acta Meteor. Sinica*, **33**, 51–63 (in Chinese).

Chen, G. T. J., and C. C. Yu, 1988: Study of low–level jet and extremely heavy rainfall over northern Taiwan in the Mei–yu season. *Mon. Wea. Rev.*, **116**, 884–891.

Chen, G. T. –J., 1977: An analysis of moisture structure and rainfall for a Mei–Yu regime in Taiwan. *Proc. Natl. Sci. Counc.*, **1(11)**, 1–21.

Deardorff, J. W., 1978: Efficient prediction of ground surface temperature and moisture, with inclusion of a layer of vegetation. *J. Geoph. Res.*, **83(4)**, 1889–1891.

Dickinson, R. E., A. Henderson–Sellers, P. J. Kennedy, and M. F. Wilson, 1993: Biosphere / Atmosphere Transfer Scheme (BATS) Version 1e as Coupled to the NCAR Community Climate Model. NCAR Tech. Note TN–387+STR, National Center for Atmospheric Research, Boulder, CO, 1–72.

Entekhabi, D., and P. Eagleson, 1989: Land surface hydrology parameterization for the atmospheric general models including subgrid–scale spatial variability. *J. Climate*, **2**, 816–831.

Famiglietti, J. S., and E. F. Wood, 1994: Multi–scale modeling of spacially–variable water and energy balance processes. *Water Resour. Res.*, **30**, 3061–3078.

Giorgi, Filippo, 1997a: An Approach for the Representation of Surface Heterogeneity in Land Surface Heterogeneity in Land Surface Models, I: Theorical frame work. *Mon. Wea. Rev.*, **125**, 1885–1899.

Giorgi, Filippo, 1997b: An Approach for the Representation of Surface Heterogeneity in Land Surface Heterogeneity in Land Surface Models, II: Validation and sensitivity experiments. *Mon. Wea. Rev.*, **125**, 1900–1919.

Holtslag, A. A. M. E. I. F de Bruijn, and H. L. Pan, 1990: A high resolution air mass transformation model for short range forcasting. *Mon. Wea. Rev.*, **118**, 1561–1575.

Holtslag, A. A. M, and B. A. Boville., 1993: Local versus nonlocal boundary–layer diffusion in global climate model. *J. Climate.*, **6**, 1825–1842.

Koster, R., and M. Suarez, 1992: Modeling the landsurface boundary in climate models as a composite of independent vegetation stands. *J. Geophys. Res.*, **97**, 2697–1715.

Leung, R. L., and S. J. Ghan, 1995: A sub-grid parameterization of orographic precipitation. *Theor. Appl. Climatol.*, **52**, 95–118.

Li, Bin, and R. Avissar, 1994: The impact of spacial variability of land surface characteristics on land-surface heat fluxes. *J. Climate.*, **7**, 527–537.

Matsumoto, S., K. Ninomiya and, S. Yosizomi, 1971: Characteristic features of "Baiu" front associated with heavy rainfalls. *J. Meteor. Soc. Japan*, **49**, 267–281.

Matsumoto, S., 1972: Unbalance low-level jet and solenoidal circulation associated with heavy rainfalls. *J. Meteor. Soc. Japan*, **50**, 194–203.

Moore, R. J., and R. T. Clarke, 1981: A distribution function approach to rainfall runoff modeling. *Water Resour. Res.*, **17**, 1367–1382.

Olson, J. S., J. A. Watts, and L. J. Allison, 1983: Carbon in live vegetation of major world ecosystems. U. S. Department of Energy, DOE / NBB-0037, No. TR004, U. S. Department of Energy, Washington, DC. 152 pp.

Seth, A., F. Giorgi, and R. E. Dickinson, 1994: Simulating fluxes from heterogeneous land surfaces: Explicit sub-grid method employing the Biosphere / Atmosphere Transfer Scheme (BATS). *J. Geophys. Res.*, **99**, 18561–18667.

Sivapalan, M., and R. A. Wood, 1995: Evaluation of the effects of general circulation model's sub-grid variability and patchiness of rainfall and soil moisture on land surface water balance fluxes. *Scale Issues in Hydrological Modeling*, J. D. Kalma and M. Sivapalan, Eds., John Wiley and Sons, 453–473.

Tao, S. Y., and L. X. Chen, 1987: A review of recent research on the East Asia summer monsoon in China. *Monsoon Meteorology*, C. P. Chang and T. N. Krishnamurti, Eds., Oxford Univ. Press, 60–92.

Wei Helin and Fu Congbin, 1997: Simulating fluxes from heterogeneous land surface. *Climat. Environ. Res.*, **2**, 107–114 (in Chinese).

Wu Yihua, and Sethu Raman, 1997: Effect of land-use pattern on the development of low-level jets. *J. Appl. Meteor.*, **36**, 573–590.